https://doi.org/10.5194/wes-2022-64
Preprint. Discussion started: 15 July 2022

WIND ENERGY SCIENCE DISCUSSIONS

Adjusted spectral correction method for calculating extreme winds in tropical cyclone affected water areas

Xiaoli Guo Larsén[1] and Søren Ott[1]

[1]Wind Energy Department, Technical University of Denmark

Correspondence: Xiaoli Guo Larsén (xgal@dtu.dk)

Abstract. A method is developed to calculate the extreme wind for tropical cyclone affected water areas. The method is based on the spectral correction method by Larsén et al. (2012) in connection with the use of numerically modeled data, where an enhancement coefficient is derived as a function of wind speed to reflect the large wind fluctuation during tropical cyclones. This is done through calibration with the estimates from Ott (2005) who used the best track data and Holland model to estimate the extreme wind over the Typhoon affected area in the western North Pacific. The method is applied in the current study to three regions where the 50-year winds with an effective temporal resolution of 10 minutes are obtained at 10 m, 50 m, 100 m and 150 m. The results are in agreement with Ott (2005) over their study domain, though with much more spatial details of the extreme wind distribution.

1 Introduction

The 50-year wind at turbine hub height (U_{50}) is one of the most important siting parameters that needs to be estimated for the wind turbine design (e.g. IEC, 2019; Yu et al., 2011). To find the correct type of wind turbines for a particular area is a necessary step for regional wind energy planning, as it is related to Levelized Cost of Energy (LCoE), that involves wind resource, safety and risk in connection with design, operation and maintenance.

Wind energy development has been expeditious in the past decade and wind turbines are being raised or planned in many regions globally, including tropical cyclone affected offshore areas.

The most reliable method to estimate U_{50} should be to use good quality measurements at the site that are sufficiently long, e.g. more than 10 years. This is however a condition that is almost never satisfied in these areas. Measurements under hurricane conditions are difficult and expensive to obtain, due mostly to technical difficulties at winds of such strength. A few meteorological stations exist in some tropical cyclone affected regions over coastal land areas. It is far from being enough for assessing the extreme conditions, particularly for over water. Moreover, most of these measurements are not accessible for general research purposes.

Alternatively, people use modeling approaches to obtain extreme wind statistics related to tropical cyclones. The often-used modeling approaches include the stochastic Monte Carlo Simulation (MCS) (e.g. IEC, 2019), the simplified physical Hurricane Holland model (Holland, 1980), and numerical Weather models.

In this study we focus on physics-based modelling approaches and therefore will not discuss MCS. In using the Holland model, Ott (2005) jointly used the best track data from 1977 to 2004 and calculated U_{50} at 10 m for the region of western North Pacific ocean; his method is referred to as the Ott method here. The values of U_{50} from Ott (2005) are of an equivalent temporal resolution of 10-min. The simple Holland model describes some of the most important parameters of a tropical cyclone, including the minimum center pressure, maximum wind speed and the distance to the cyclone eye. It also assumes a spatially symmetric distribution of wind speed from the cyclone eye to outer region. The simplicity of the Ott method at the same time caused its limitation, e.g. the lack of detailed spacial information of the wind speed, horizontally and vertically. Moreover, the Ott method needs feed-in information of the best track data.

Numerical modeling has been a powerful tool in simulating tropical cyclones, as being done in research and forecasting centers for Hurricanes and Typhoons. These weather models can be run at a spatial resolution from a few kilometers to a few tens of kilometers, with outputs most-often saved hourly. These long-term simulation data are valuable for the assessing the extreme wind in tropical cyclone affected areas. However, most of these simulations are forecast with model schemes and setups that undergo regular and continuous updates and improvement. The updates are advantageous for forecasting purposes, but not necessarily for calculating the extreme winds, because inconsistency is introduced into the long-term data, which will affect the extreme wind samples artificially. Moreover, the data from weather centers are not always accessible for wind energy users.

The reanalysis data thus have been a very attractive option, as they are generated using a consistent setup and they are globally available with open access. Some of them, e.g. Climate Forecast System Reanalysis (CFSR) and the fifth generation ECMWF reanalysis (ERA-5) are of spatial resolution of about 25 - 40 km, available at hourly basis. For instance, Pryor and Bartelmie (2021) has used the ERA-5 data and created a global atlas of extreme wind at 100 m. However, their data validation suggests that the extreme winds in tropical cyclone affected areas are significantly underestimated. This is nevertheless expected, as Larsén et al. (2012) showed through spectral analysis of the modeled wind speed time series. Wind time series from mesoscale numerical models in general suffers from the numerical smoothing effect, where the smoothing was used for numerical stability of the modeling. Larsén et al. (2012) showed that the modeled time series misses the high-frequency variability in comparison with measurements of similar resolution, causing systematic underestimation of the 50-year wind. This is the case almost ever-present in data from mesoscale modeling, and the smoothing effect is expected to be significant for reanalysis data of tens of kilometers spatial resolution. To solve this problem, Larsén et al. (2012) developed a so-called spectral correction (SC) method to fill in the missing wind variability to modeled time series through a spectral model, thus the corrected time series will have the power spectrum matching the measurements of a given resolution. To meet the IEC standards, we can correct the spectrum to an equivalent resolution of 10 min. This SC method is briefly introduced in section 2.2 here.

The SC method has been used in connection with different reanalysis data to create extreme wind globally, including CFSR and Climate Four-Dimensional Data Assimilation (CFDDA) (Larsén and Kruger, 2014; Hansen et al., 2016; Larsén et al., 2022). The SC method has been shown to be reliable when validated with mid-latitude measurements. However, applying SC in the same way as for the mid-latitude storms suggests a significant underestimation of U_{50} for the western north Pacific Ocean, when comparing with the results from Ott (2005).

The current study provides a simple approach for all tropical cyclone affected water areas, combining the strengths of the Ott method and the SC method from Larsén et al. (2012). This method is denoted here as the spectral correction for tropical cyclone method, in short, the SC-TC method.

This new method is described in section 2. Section 3 shows results with discussions for the western Pacific Ocean as well as two other regions that are under the impact of tropical cyclones. Conclusions are provided in section 4.

2 The development of the method

2.1 The data

In this study, in connection with the development of the SC-TC method, we have used the wind speed at 10 m from CFSR-1 reanalysis data. The CFSR-1 data are available from 1979 - 2010, and they are hourly values at a spatial resolution of about 40 km (Saha et al., 2010). There is a version-2 CFSR data, CFSv2, which are available from 2011, with a higher spatial resolution of about 25 km. However, the total data length of CFSv2 is too short for the calculation of the 50-year wind. The CFSv2 data are however, used to investigate the wind speed spectra during a Typhoon case Megi in section 2.2. Outputs for Megi from the mesoscale Weather Research and Forecasting (WRF) model, with a spatial resolution of 2 km, are also used.

When developing the SC-TC method, we also used the estimation of the 50-year wind at 10 m from Ott (2005), which were from the best track data and Holland model, for one area over the western north Pacific ocean. These values, called here $U_{50,Ott}$, are available on grid size of about 1°. They are from Fig. 13 in Ott (2005) and re-produced here in contour lines in Fig. 3a.

2.2 The SC–TC method

As explained in Section 1, the smoothened time series from numerical models results in missing wind variability and accordingly low spectral energy, at higher frequencies, when compared to measurements (Larsén et al., 2012). Fig. 1 shows an example of the spectrum from modeled time series (black curve, from the 32-year CFSR-1 data) in comparison with expected spectral tail that has a slope of $-5/3$ in a log-log coordination (solid red curve).

The effect of the smoothing of the time series on the estimation of the extreme wind is calculated in Larsén et al. (2012) by assuming that the once-per-year exceedance follows a Poisson process. The maximum wind that occurs once a year $\overline{U}_{\max}$ was derived as a function of the zero- and second-order spectral moments m_0 and m_2:

$$\overline{U}_{\max} = \overline{U} + \sqrt{m_0}\sqrt{2\ln\left(\frac{1}{2\pi}\sqrt{\frac{m_2}{m_0}}T_0\right)} \qquad (1)$$

where $\overline{U}$ is the mean wind speed, T_0 is the basis period of one year and m_i is the ith spectral moment defined by

$$m_i = 2\int_0^\infty f^i S(f)\,df \tag{2}$$

where f is the frequency in Hz and $S(f)$ is the spectrum of the wind speed. From the above equations, it is clear that $\overline{U}_{\max}$ is significantly affected by the high frequency part of the spectrum through m_2. Thus, we can improve the calculation of $\overline{U}_{\max}$ by correcting the spectral tail.

Such a correction has been done by replacing the high frequency part of the spectrum from the modeled time series with the following spectral model:

$$S(f) = a \cdot f^{-5/3} \tag{3}$$

from a certain frequency f_c to the expected frequency f_h. In our study it is the 10-min temporal resolution we aim at, so that $f_h = 72$ day^{-1} (0.00083 Hz), which is the Nyquist frequency for 10-min. Eq. 3 is the mesoscale part of the expression from Larsén et al. (2013), which includes both a synoptic and mesoscale range of spectrum: $S(f) = a \cdot f^{-5/3} + b \cdot f^{-3}$. As shown by Fig. 1, a is determined by the time series of the model data where the black curve and the red solid curve meet. In Hansen et al. (2016), $f_c = 0.8$ day^{-1} was used. In Larsén et al. (2022), f_c and $S(f_c)$ were chosen from a regression line of $\ln S(f)$ with $\ln f$ for the range $0.6 < f < 0.9$ day^{-1}, thus the choice of f_c becomes less sensitive to the fluctuation in $S(f)$.

The SC method was shown to provide reasonable estimates for mid-latitude storms (e.g. Hansen et al., 2016; Larsén and Kruger, 2014). However, using Eq. 3 results in underestimation of U_{50} for the tropical cyclone affected areas. It is because the energy level in the mesoscale range during tropical cyclones is significantly higher. This is demonstrated in Fig. 2 through an example of spectral analysis during typhoon case Megi that past Taiwan during the period 26th - 27th Sep. 2016. It is not the focus of current study to investigate mesoscale modeling of the tropical cyclones, thus, details of the simulation of typhoon Megi using the WRF model are given in Appendix A. As the period is too short for a Fourier analysis of the time series in time domain, we examine the power spectra in wavenumber domain, namely, $E(k)$ vs. wavenumber (k). We compare the spectral behaviour and energy level for the wind speed between this particular case and climatological conditions in Fig. 2. Here the climatological condition is represented by two data sources, one with the CFSv2 data of the entire year 2016 (green curves), and the other as the wavenumber spectrum from Gage and Nastrom (1986) (the black curve). Spectra $E(k)$ corresponding to Megi were calculated over an area of about 200 km by 200 km over the Pacific Ocean as Megi approached Taiwan during the period 2016-09-26 10:00 to 2016-09-27 09:00; both the reanalysis data CFSv2 (blue in Fig. 2) and the WRF data were used (red). We calculated and averaged the one-dimensional spectra in the North-South (N-S) direction as well as West-East (W-E) direction. They are plotted as solid and dashed curves, respectively, in Fig. 2. Thus, the spectra represent an average energy level over the entire area, which is more representative for this particular case in comparison with a spectrum derived with time series at certain grid point. For the climatological condition, the energy level and spectral slope are similar for the overlapping wave number range between the 1-year CFSR-1 data and the spectrum of Gage and Nastrom (1986), and both have significantly lower energy level than that for the Megi case. For this particular case, the higher resolution WRF-SWAN simulation contributed to spatial wind variability that is about 3 - 5 times larger than the CFSv2 data (about 25 km).

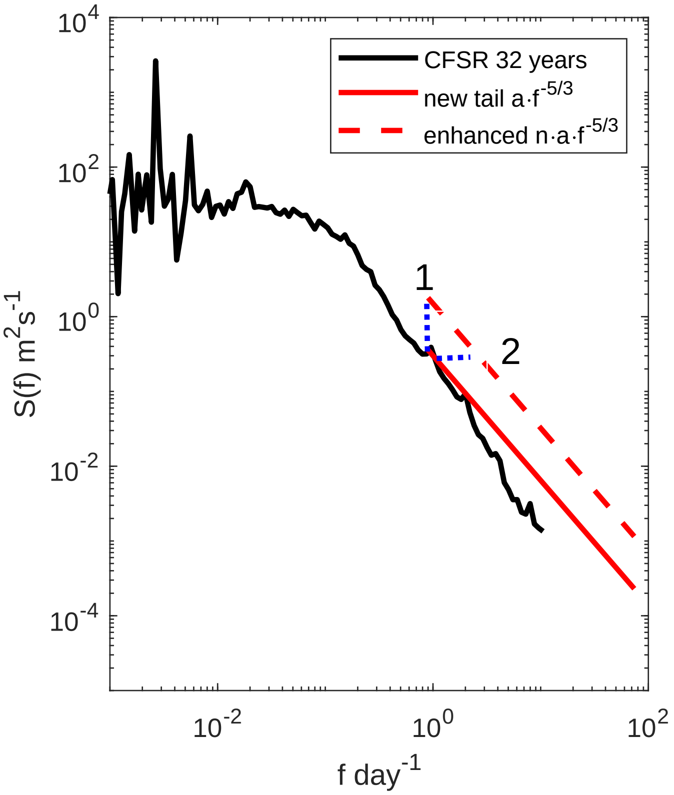

Figure 1. Illustration of extending the SC method to the SC-TC method, where the black curve shows the wind speed spectrum from the model data (here, 32-year CFSR-1 wind speed at 10 m), the red solid curve is Eq. 3 and the red dashed curve is Eq. 4. The two blue dotted lines suggest two possible ways of connecting the red curves to the original spectrum for the spectral correction.

120 To adjust the SC method for more general storm conditions, we revise Eq. 3 to

$$S(f) = n \cdot a \cdot f^{-5/3} \tag{4}$$

with n a coefficient reflecting weather types and its value can be adjusted with additional data, e.g. measurements. Thus for mid-latitude storms, $n = 1$, and for tropical cyclones, we develop a systematic way to determine n, which is described in the following. Here we need to decide how to link the new spectral tail (red dashed curve in Fig 1) to the long term spectrum (the 125 black curve). In Fig 1, the two blue dotted curves, labelled as 1 and 2, suggest two possible ways of introducing the red dashed curve to the calculation. To keep it simple and to be on the conservative side, we use the blue line number 1 to proceed with the calculation.

In finding n in Eq. 4, firstly, 32-year annual maximum winds u_{max} are extracted from the CFSR-1 data from 1979 to 2010. The 50-year wind at its original resolution, $U_{50,uncorr}$, are calculated applying the Gumbel distribution to the 32 values with 130 the Annual Maximum Method (e.g. Abild et al., 1992; Larsén et al., 2019). Secondly, we use the results of the 50-year wind

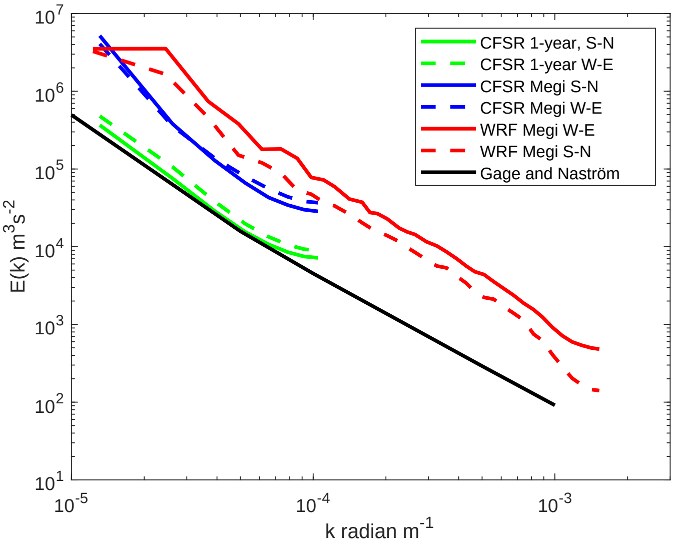

Figure 2. Power spectrum of wind speed over the space $E(k)$ as a function of wave number k, demonstrating higher spectral energy level associated with tropical cyclones in comparison with climatological conditions, with an example from Typhoon Megi. Here the $k-$spectra calculated from the WRF modeling and from CFSv2 data during Typhoon Megi for 2016-09-26 10:00 to 2016-09-27 09:00 over water are compared with the spectra from one-year of CFSv2 data (2016) and the climatologically representative spectrum from Gage and Nastrom (1986).

from Ott (2005), $U_{50,Ott}$ (see section 2.1), to train the CFSR-1 data. We re-grid $U_{50,Ott}$ (spatial resolution of 1°) to the CFSR-1 model grids (spatial resolution of about 40 km) and calculate the ratio $r = U_{50,Ott}/U_{50,uncorr}$. The distribution of r with $U_{50,Ott}$ is shown in Fig. 4a in gray dots. The values of r range from about 1 to 2.6. By varying n in Eq. 4 in connection with the use of the SC method, different U_{50} are obtained. Here, to match the IEC requirement, as also applied in Ott (2005), we correct 135 the values to the equivalent 10-min resolution, hence $f_h = 72$ day^{-1} is used. By comparing the estimates to the corresponding $U_{50,Ott}$, a relation between n and r can be established. This relation depends on the location of interest in relation to the tropical cyclone structure, with n increasing faster with r for stronger wind regions. In theory, such a relation can be derived for all grid points. As we do not always have the best track data for a given location, to be on the conservative side, we use the $n-r$ relation from the grid point (17N, 130E), which corresponds to the strongest winds in the region based on the CFSR data. 140 A look up table can eventually be derived for the relationship between n and annual wind maximum u_{max}. The relationships read:

$$
\begin{aligned}
n &= 1, \quad r \leq 1.118 \\
&= \alpha r^2 + \beta r + c, \quad r > 1.118
\end{aligned}
\tag{5}
$$

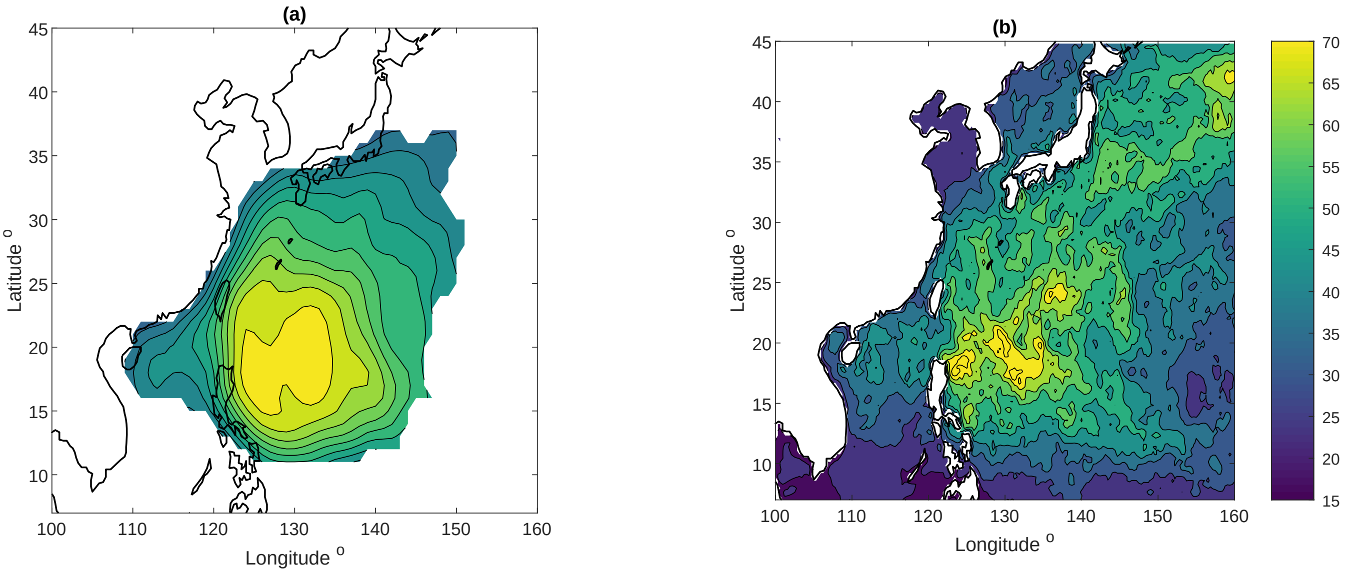

Figure 3. Spatial distribution of the 10-min 50-year wind at 10 m over southern North Pacific ocean. (a) re-produced with data from Fig. 13 in Ott (2005); (b) from the SC-TC method developed here.

where $\alpha = 37.83$, $\beta = -55.08$ and $c = 15.27$ were obtained based on the grid point (17N, 130E), with

$$\begin{aligned} r &= 1.11, \quad u < 27.5 \\ &= 0.017u + 0.65, \quad 27.5 \leq u < 60 \\ &= 1.67, \quad u \leq 60 \end{aligned} \tag{6}$$

With u the input of the annual wind maxima, n can be obtained. For annual wind maximum u_{max} smaller than 27.5 m s^{-1}, $n = 1$, same as Eq. 3. Thus, the SC-TC method is ready to be used and it merges with the SC method for $u_{max} < 27.5$ m s^{-1}. Fig. 4b shows the inter-relationship between n, r and u.

2.3 Extreme wind at different heights

Usually, model wind outputs are provided at a few certain heights, e.g. 10 m or 100 m, and most models provide outputs at 10 m. The calculation of U_{50} in Ott (2005) is at height $z = 10$ m, and the CFSR-1 data we used so far are also at 10 m. Modern offshore wind turbines can be as tall as a couple of hundreds of meters. We introduce a simple approach here to obtain winds at other heights U_z from 10-m winds for storm conditions.

In extreme wind conditions, the logarithmic wind law can be considered valid up to several hundreds of meters according to the Sonde wind speed measurements during hurricane conditions as shown in e.g. Powell et al. (2003); Giammanco et al.

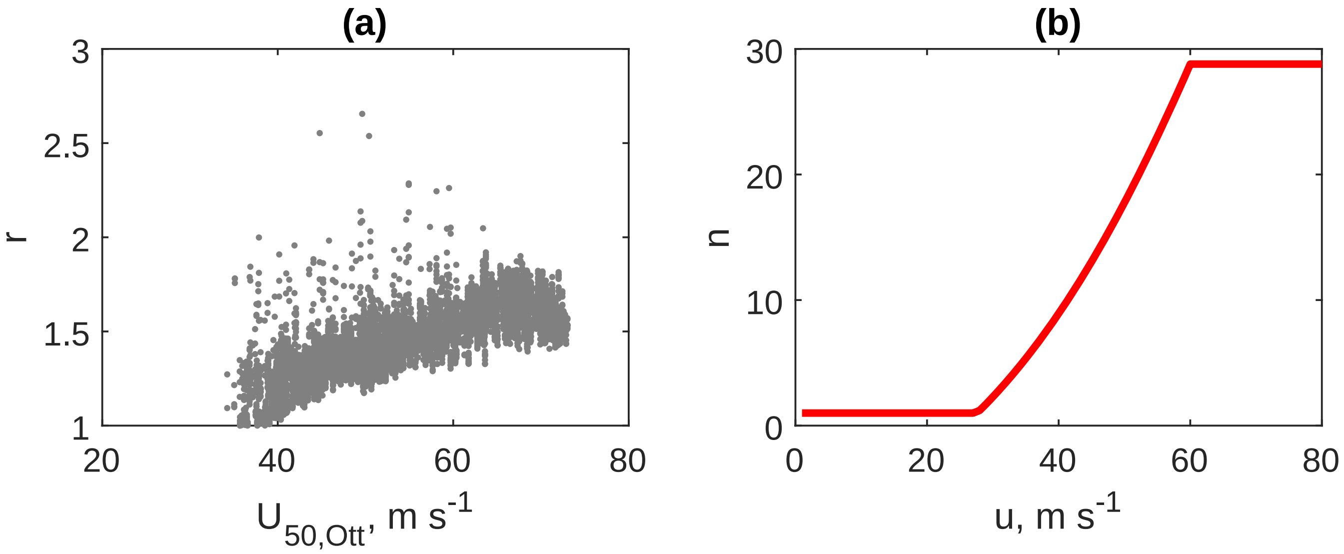

Figure 4. (a) The distribution of the ratio of the 50-year wind from the CFSR-1 data and $U_{50,ott}$ from Ott (2005), r, with $U_{50,ott}$; (b) The derived dependence of n on r as in Eq. 4.

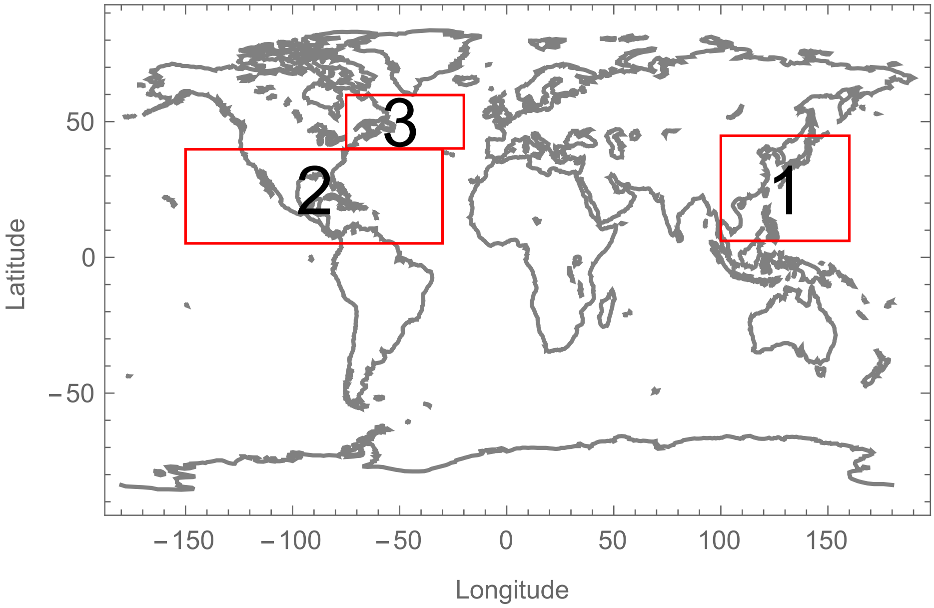

Figure 5. The three regions chosen for the calculation of the extreme wind using the SC-TC method.

(2013). Thus we can calculate U_z using

$$U_z = (u_*/\kappa)\ln(z/z_0). \tag{7}$$

where u_* is the frictional velocity. With U_{10m} at $z = 10$ m known, U_z can thus be obtained analytically if we have one more relation for z_0 and u_*.

There are several such relations established in the literature for describing z_0 and u_*. Here we examined three of them, with the first one the Charnock formulation for well-developed wind sea waves (Charnock, 1955) :

$$z_0 = \alpha_{ch} u_*^2/g, \tag{8}$$

where α_{ch} is the Charnock coefficient, which depends on the sea state, and it is larger for rougher sea. In numerical models, it is often between 0.011 to 0.02, as a function of wind speed. Here for the strong winds, we use $\alpha_{ch} = 0.02$.

The second one is the Andreas algorithms that take into account of spray effect at strong wind conditions (Andreas et al., 2015):

$$u_* = 0.239 + 0.0433\left((U_{10m} - 8.271) + \left(0.12(U_{10m} - 8.271)^2 + 0.181\right)^{0.5}\right),$$
$$z_0 = 10\exp\left(-\kappa U_{10m}/u_*\right). \tag{9}$$

And the third are the algorithms that are used in wave model SWAN (e.g. Zijlema and van der Westhuysen, 2005). The SWAN algorithms are based on field measurements over a wide range of wind speed conditions, including hurricane conditions. It suggests a level-off or decreasing of surface drag coefficient (C_d) or roughness length with wind speed at strong winds, interpreted as a result from wave breaking processes:

$$C_d = \left(0.55 + 2.97(U_{10m}/31.5) - 1.49(U_{10m}/31.5)^2\right)10^{-3},$$
$$u_* = \sqrt{C_d}U_{10m},$$
$$z_0 = 10\exp\left(-\kappa U_{10m}/u_*\right). \tag{10}$$

In a test of calculating the wind speed at 100 m using wind speed at 10 m, it is found that the difference in using the three above-mentioned formulations is negligible for winds at 100 m up to 25 m s^{-1}. While the Charnock formulation with $\alpha_{ch} = 0.02$ gives very similar results to the Andreas formulation up to 40 m s^{-1}, it provides larger values for stronger winds, with the difference of about 1 m s^{-1} at 50 m s^{-1}. Both the Charnock and the Andreas formulations give larger estimations than the SWAN formulations for winds larger than 25 m s^{-1}, and the overestimation increases to about 3 m s^{-1} at 50 m s^{-1}. In this study we proceed our calculation using the SWAN formulation as it provides surface wave breaking effect at strong winds, which is calibrated with measurements (though very few) during hurricane conditions. We note that all of these formulations are over-simplification of the sea surface at such strong wind conditions during tropical cyclones and uncertainty is embedded.

3 Results and discussions

The SC-TC method is applied to three areas in this study and they are marked in Fig. 5 in boxes, with box-1 covering the same region as in Ott (2005) for typhoons and boxes 2 and 3 for hurricanes. Three areas are chosen as they host the most severe and frequent tropical cyclones, based on the International Best Track Archive from National Centers for Environmental Information (NOAA) (https://www.ncei.noaa.gov/news/inventory-tropical-cyclone-tracks).

For the three areas, the 50-year winds are calculated at 10 m, 50 m, 100 m and 150 m. With values at the four heights available, one can also obtain values at any height in-between using an interpolation or extrapolation method, e.g. polynomial. The data of these 50-year winds at the four heights are provided in the database https://zenodo.org/record/6604117#.YpeznXVBxaQ.

In order to compare with the result from Ott (2005) (re-produced here as Fig. 3a), U_{50} at 10 m from the SC-TC method is presented at Fig. 3b. From Fig. 3, one can see that, first of all, the wind speed range is comparable for the common area of the two plots, being from about 35 to 70 m s^{-1}. Secondly, the locations of the strongest winds are consistent in the two plots, being between $120-140°$E and $15-25°$N. The contour lines in Fig. 3a are very smooth due to the use of Holland model and coarse resolution best track data (1°) in the Ott method, while Fig. 3b reveals richer spacial details. The agreement between Fig. 3a and b is an encouragement to apply the SC-TC method to other tropical cyclone affected areas. Figure 6 shows 10-min U_{50} at 100 m, which is a more relevant height for modern offshore turbines.

Even though we have used the CFSR-1 data in this paper, the SC-TC method can be applied similarly with other reanalysis data with sufficient data length. Though the quality of the reanalysis data, including the information of tropical cyclone parameters such as path, intensity and spatial structures, needs to be quality checked first. Imberger and Larsén (2022) shows that the characteristics of tropical cyclones are quite different in the following reanalysis data: CFSR-1, MERRA-2 (Modern-Era Retrospective analysis for Research and Applications), ERA-5 and CFDDA. For instance, among the four, the patterns of tropical cyclones are very weak in the CFDDA data. This also suggests a source to uncertainty, or error, to the estimation through the model data that is used.

Note that the three boxes do not include all areas with the impact of tropical cyclones. Note also that the current study only addresses “water areas”; this is mainly because of two reasons. Firstly, extrapolation of surface winds to other heights over land requires much more complicated modeling approaches due to spatial inhomogeneous surface conditions. Moreover, it is not a trivial task to obtain such data for the surface conditions, whereas over water we benefit from the dependence of roughness length on the wind speed, even though there is uncertainty introduced. In addition, the best track data used for calibration in connection with the SC-TC method is mostly available over water.

It should be pointed out that using the dependence of n on the only parameter, wind speed, results in that we are using the SC-TC method to strong wind regions that might not be “tropical cyclone affected”. It can be improved with further input of information when possible, to indicate if it is an area with tropical cyclone impact or not. In addition, the use of Eq. 4 has now been calibrated for mid-latitude storms and tropical cyclones, it is not yet examined for other types of extreme wind events such as thunderstorms; further studies are needed to extend the application of the method.

In spite of the uncertainties, the method and the data produced in this study serve to fill in the void of extreme wind estimations in most tropical cyclone affected areas. We acknowledge that we do not have enough measurements for validation, other than the study of Ott (2005), and therefore encourage validation from measurement owners.

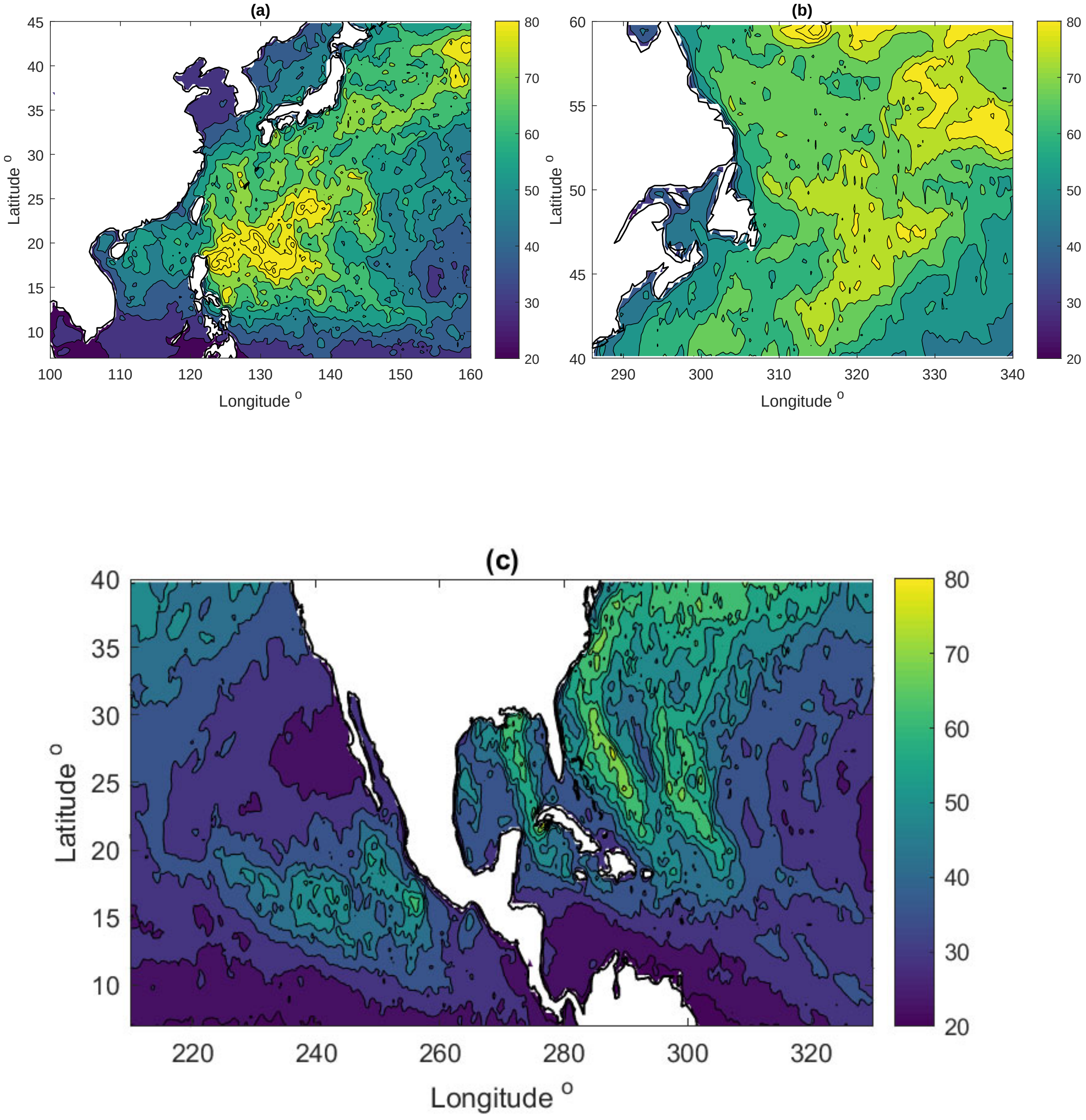

Figure 6. The 50-year wind of 10-min values at 100 m over water in three zones as in Fig. 5.

https://doi.org/10.5194/wes-2022-64
Preprint. Discussion started: 15 July 2022

4 Conclusions

This study develops a method for calculating the extreme wind for tropical cyclone affected areas, here called the SC-TC method. This is done by adjusting the spectral correction (SC) method from Larsén et al. (2012), through adding an enhancement coefficient to the spectral model, with the coefficient dependent on the local extreme wind. Such a dependence is calibrated using the estimates from Ott (2005) who used the best track data and Holland model for the area of southern North Pacific ocean. The results from the SC-TC method provide consistent wind distribution of 10-min 50-year wind at 10 m, and in addition much richer and more realistic spatial details, in comparison with the results from Ott (2005). The method can be applied for all water areas with tropical cyclones and can be used to obtain extreme winds from surface to a few hundreds of meters.

Data availability. The CFSR data are publicly available at https://rda.ucar.edu/. The 50-year wind values over the three areas at 10 m, 50 m, 100 m and 150 m are available at https://zenodo.org/record/6604117#.YpeznXVBxaQ, doi:10.5281/zenodo.6604117

Appendix A: Mesoscale modeling of typhoon Megi using WRF

There are two purposes of using the mesoscale Weather Research and Forecasting (WRF) model. The first is to examine the spectral energy level during an example case of typhoon in comparison of climatological conditions. The second is to compare the spectral energy level from the CFSv2 data (with a spatial resolution of tens of kilometers) with that from the WRF data (with a spatial resolution of 2 km).

We used WRF version 4.0, configured with the moving nest function. Three nested domains are used, with spatial resolutions of 18 km, 6 km and 2 km, respectively. The innermost domain has 339 by 342 grid points. We used 52 vertical model levels from surface to pressure level of 5000 Pa. We used the new Thompson microphysics scheme (Thompson et al., 2004), the RRTMG scheme for long and short wave radiation physics scheme (Iacono et al., 2008), MYNN 3.0 PBL scheme (Nakanishi and Niino, 2009) and Noah Land Surface Model. The Kain-Fritsch cumulus scheme (Kain and Fritsch, 1993) was used for the outer domain (I) but not for domains II and III. We used ERA5 data as the initial and boundary forcing for WRF. The daily 0.25° OISST data were used. The simulation started at 26th Sep. 2016 00:00 and ends at 27th Sep. 2016 12:00, with the first 12 hours as spinning-up period. The model outputs are every 10 min.

Figure A1 shows the typhoon track from three data sources, the best track data, the CFSv2 data as the position of the lowest mean sea level pressure (MSLP) and the WRF data, also as the position of the lowest MSLP. They are in good agreement.

Both the wind speed data from CFRv2 and WRF from 12:00 on 26th to 12:00 on 27th over the innermost model domain are used to obtain the mean spectra of the longitudinal and meridional wind as shown in Fig. 2.

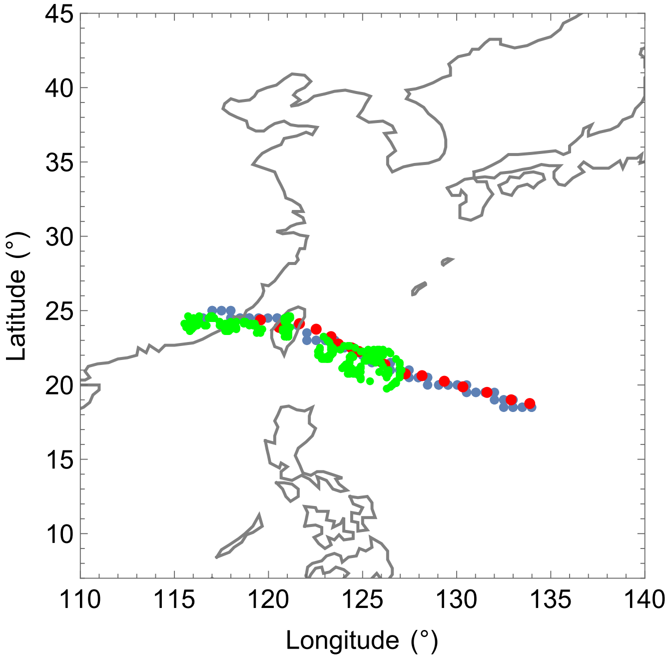

Figure A1. Center positions (with lowest mean sea level pressure) and track of Typhoon Megi in September 2016, red: best track data (23rd - 26th Sep. 2016); blue: CFSv2 data (23rd - 27th Sep. 2016); green: WRF data (26rd - 27th Sep. 2016).

250 *Author contributions.* XL outlined the paper, developed the SC-TC model and did the calculation. SO provided data from Ott (2005) and suggestions. XL wrote the paper with suggestions from SO.

Competing interests. The authors declare that they have no conflict of interest.

Acknowledgements. This study is supported by the EUDP projects GASP (EUDP J. nr. 64018-0095) and GASPOC (EUDP J. nr. 65020-1043). The CFSR products are downloaded from https://rda.ucar.edu/.

https://doi.org/10.5194/wes-2022-64
Preprint. Discussion started: 15 July 2022

References

Abild, J., Mortensen, N., and Landberg, L.: Application of the wind atlas method to extreme wind speed data, J. Wind Eng. Ind. Aerodyn., 41, 473–484, 1992.

Andreas, E. L., Mahrt, L., and Vickers, D.: An improved bulk air-sea surface flux algorithm, including spray-mediated transfer, Q.J.R. Meteorol. Soc., 141, 642–654, https://doi.org/10.1002/qj.2424, 2015.

Charnock, H.: Wind stress on a water surface, Q. J. R. Meteorol. Soc., 81, 639–640, 1955.

Gage, K. and Nastrom, G.: Theoretical interpretation of atmospheric wavenumber spectra of wind and temperature observed by commercial aircraft during GASP, J. Atmos. Sci., 43, 729–740, 1986.

Giammanco, I. M., Schroeder, J. L., and Powell, M. D.: GPS Dropwindsonde and WSR-88D Observations of Tropical Cyclone Vertical Wind Profiles and Their Characteristics, Weather and Forecasting, 28, 77 – 99, https://doi.org/10.1175/WAF-D-11-00155.1, 2013.

Hansen, B. O., Larsén, X. G., Kelly, M., Rathmann, O. S., Berg, J., Bechmann, A., Sempreviva, A. M., and Jørgensen, H. E.: Extreme wind calculation applying spectral correction method - test and validation, Tech. rep., Wind Enery Department, Technical University of Denmark, DTU Wind Energy E-0098, 2016.

Holland, G.: An analytic model of the wind and pressure profiles in hurricanes, Mon. Wea. Rev., pp. 1212–1218, 1980.

Iacono, M. J., Delamere, J. S., Mlawer, E. J., Shephard, M. W., Clough, S. A., and Collins, W. D.: Radiative forcing by long-lived greenhouse gases: Calculations with the AER radiative transfer models, Journal of Geophysical Research, 113, 13 013, 2008.

IEC: IEC 61400-1 Ed4: Wind turbines - Part 1: Design requirements, standard, International Electrotechnical Commission, Geneva, Switzerland, 2019.

Imberger, M. and Larsén, X. G.: Sensitivity and quality assessment of global 50-year return winds using reanalysis products and measurements, WindEurope, https://windeurope.org/annual2022/conference/posters/PO254/, 2022.

Kain, J. S. and Fritsch, J. M.: Convective parameterization for mesoscale models: The Kain-Fritsch scheme. The representation of cumulus convection in numerical models, Meteor. Monogr., Ameri. Meteor. Soc., 24, 165–170, 1993.

Larsén, X. G. and Kruger, A.: Application of the spectral correction method to reanalysis data in South Africa, J. Wind Eng. Ind. Aerodyn., 133, 110–122, 2014.

Larsén, X. G., Du, J., Bolaños, R., Imberger, M., Kelly, M. C., Badger, M., and Larsen, S.: Estimation of offshore extreme wind from wind-wave coupled modeling, Wind Energy, 22, 1043–1057, https://doi.org/10.1002/we.2339, 2019.

Larsén, X. G., Ott, S., Badger, J., Hahmann, A. H., and Mann, J.: Recipes for correcting the impact of effective mesoscale resolution on the estimation of extreme winds, J. Appl. Meteorol. Climat., 51, 521–533, https://doi.org/10.1175/JAMC-D-11-090.1, 2012.

Larsén, X. G., Vincent, C. L., and Larsen, S.: Spectral structure of the mesoscale winds over the water, Q. J. R. Meteorol. Soc., 139, 685–700, https://doi.org/DOI:10.1002/qj.2003, 2013.

Larsén, X. G., Davis, N., Hannesdottir, , Kelly, M., Svenningsen, L., Slot, R., Imberger, M., Olsen, B., and Floors, R.: The Global Atlas for Siting Parameters (GASP) project: extreme wind, turbulence and turbine classes, Wind Energy, Accepted, 2022.

Nakanishi, M. and Niino, H.: Development of an improved turbulence closure model for the atmospheric boundary layer, J. Meteorol. Soc. Jpn, 87, 895–912, 2009.

Ott, S.: Extreme winds in the western North Pacific, Tech. Rep. Risoe-R-1544(EN), Risø National Laboratory, Roskilde, Denmark, URL:www.risoe.dk/rispubl/VEA/veapdf/ris-r-1544.pdf, 2005.

Powell, M. D., Vickery, P. J., and Reinhold, T. A.: Reduced drag coefficient for high wind speeds in tropical cyclones, Nature, 422, 279–283, 2003.

Pryor, S. and Bartelmie, R. J.: A global assessment of extreme wind speeds for wind energy applications, Nature Energy, https://doi.org/https://doi.org/10.1038/s41560-020-00773-7, 2021.

Saha, S., Moorthi, S., Pan, H.-L., Wu, X., Wang, J., Nadiga, S., Tripp, P., Kistler, R., Woollen, J., Behringer, D., Liu, H., Stokes, D., Grumbine, R., Gayno, G., Wang, J., Hou, Y.-T., ya Chuang, H., Juang, H.-M. H., Sela, J., Iredell, M., Treadon, R., Kleist, D., Delst, P. V., Keyser, D., Derber, J., Ek, M., Meng, J., Wei, H., Yang, R., Lord, S., van den Dool, H., Kumar, A., Wang, W., Long, C., Chelliah, M., Xue, Y., Huang, B., Schemm, J.-K., Ebisuzaki, W., Lin, R., Xie, P., Chen, M., Zhou, S., Higgins, W., Zou, C.-Z., Liu, Q., Chen, Y., Han, Y., Cucurull, L., Reynolds, R. W., Rutledge, G., and Goldberg, M.: The NCEP Climate Forecast System Reanalysis, Bulletin of the American Meteorological Society, 91, 1015 – 1058, https://doi.org/10.1175/2010BAMS3001.1, 2010.

Thompson, G., Rasmussen, R. M., and Manning, K.: Explicit forecasts of winter precipitation using an improved bulk microphysics scheme. Part-I: Description and sensitivity analysis, Mon. Weather Rev., 132, 519–542, 2004.

Yu, Q., Kim, K., and Lo, T.: Design Standards for Offshore Wind Farms, Tech. rep., American Bureau of Shipping, contract M10PC00105, 2011.

Zijlema, M. and van der Westhuysen, A. J.: On convergence behaviour and numerical accuracy in stationary SWAN simulations of nearshore wind wave spectra, Coastal Engineering, 52, 237–256, https://doi.org/10.1016/j.coastaleng.2004.12.006, 2005.